Supporting Information

Spiro-[4,5]-cyclohexadiene-8-one Polymers: Photoactivated Crosslinking and Switch-On Fluorescence for Lithography

Yi Yuan, [†a] Mi Chao, [†a] Yunyi Shang,[a] Yujia Gao,[a] Guangle Niu[b], Wanggang Fang[c], Liqing He*[c], Hui Wang*[a]*

[a]Key Laboratory of Synthetic and Natural Functional Molecule Chemistry of the Ministry of Education, College of Chemistry & Materials Science, Northwest University, Xi'an 710127, China.

[b]School of Chemistry and Chemical Engineering, Beijing Institute of Technology, Beijing 100081, China

[c]Hefei General Machinery Research Institute Co., Ltd., Hefei 23000, Anhui, China

1. General information

1.1. Materials

All reactions were carried out under an argon atmosphere using standard Schlenk-Lines or glovebox (Innovative Technology). DCM were dried over calcium hydride. If not specifically mentioned, all chemicals were used as received from Sigma-Aldrich Corporation, Innochem and without further purification. Analytical thin-layer chromatography was performed with 0.25 mm coated commercial silica gel plates (TLC Silica Gel 60 F_{254}); visualization of the developed chromatogram was performed by fluorescence. Flash chromatography was performed with silica gel (300-400 mesh).

1.2. Instruments

Nuclear magnetic resonance (NMR) spectroscopy

Proton nuclear magnetic resonance (^{1}H NMR) data were acquired on Bruker Ascend 400 (400 MHz) spectrometer. Chemical shifts are reported in delta (δ) units, in parts per million (ppm) downfield from tetramethylsilane. Coupling constants J are quoted in Hz. Carbon-13 nuclear magnetic resonance (^{13}C NMR) data were acquired at 101 MHz on Bruker Ascend 400 spectrometer. The chemical shift references were as follows: for ^{1}H NMR spectra, Chloroform-*d* at 7.260 ppm, $(CD_3)_2SO$ at 2.05 ppm and for ^{13}C NMR spectra, Chloroform-*d* at 77.0 ppm, $(CD_3)_2SO$ at 39.5 ppm.

High resolution mass spectra (HRMS)

HRMS were acquired on a Bruker Daltonics MicroTof-Q II mass spectrometer.

Fourier transform infrared spectroscopy (FT-IR)

FT-IR was performed using an INVENIO spectrometer (Bruker, Germany). Grind 1 mg sample with 100 mg KBr, press it into a transparent wafer and measure it in the range of 500-4000 cm^{-1}.

Gel permeation chromatography (GPC)

Regarding gel permeation chromatography (GPC), the analysis was performed using Agilent GPC-1260 liquid chromatography THF phase, including PL1110-6100 mixed gel column (10 μm; 300 ∅ 7.5 mm) and PL1110-6540 column (5 μm; 300 ∅ 7.5mm). The flow rate is 1.0 mL min^{-1} (25 °C). Calibrate column chromatography using standard polystyrene (PSt) from THF phase, and obtain a standard calibration curve for PMMA by converting with the Mark-Houwink Equation.

Rheological analysis

Rheological analysis was performed in an Anton Paar MCR 302 rheometer equipped with a parallel plate configuration (25 mm diameter). The data was analysed using the RheoCompass software.

Thermogravimetric analysis (TGA)

The TGA measurements were performed using a STA 449C (Netzsch Co., Germany) under nitrogen atmosphere at a flow rate of 10 mL min^{-1}.

Differential scanning calorimetry (DSC)

The DSC measurements were carried out using a TA Instruments DSC 2910 thermal analyzer at a heating rate of 10 °C min^{-1}.

Ultraviolet-Visible (UV-Vis) spectra

The UV-Vis spectra were determined on a Hitachi U-2900 spectrometer.

Photoluminescence (PL) spectra

Fluorescence spectra were acquired on a Hitachi F-4500 fluorescence spectrometer with a 10-mm quartz cuvette.

Ultraviolet light source

At room temperature, the polymer film was photocrosslinked by UV light (365 nm, 10 mw/cm^2) through the photomask, the irradiation distance was 3.5 cm and the fluorescence pattern was generated. The light source is a portable ultraviolet analyzer, instrument model WHF-204BS.

Film and photomask making

A silicon wafer (25 mm $\varnothing$ 25 mm) with a clean and flat surface was immersed in a chloroform solution of **P1/2a** (50 mg/mL). The silicon wafer coated with polymer solution is left for 12 h to evaporate the solvent to form a solid film. Then dry in a 70 ℃ oven for 2 hours. The "NWU" and "flower" photomask are cut from a piece of black paper and glued to a quartz sheet (25 mm $\varnothing$ 25 mm). A photomask with a "circular" pattern is a precision metal mask with a hollow circle with a diameter of 100 μm.
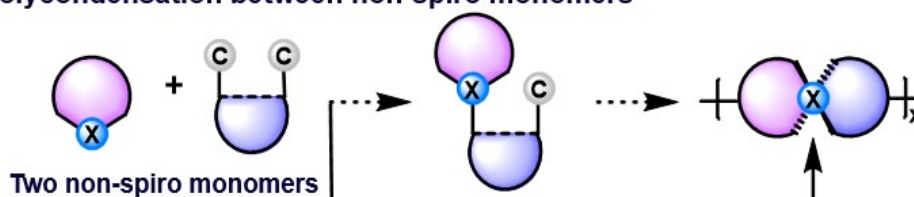
2. Synthesis of spiropolymers

(a) Preparation of pre-synthesized spiro monomers

Spiro monomers **Comonomer**
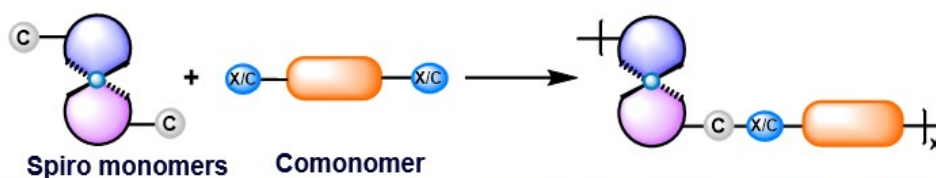
- Prefabricated spiro monomers
- Difficult to introduce multiple substituents
- Well-designed comonomer
- Cumbersome reaction process

(b) Polycondensation between non-spiro monomers

Two non-spiro monomers

- Limited monomer structure
- Few reaction types
- Poor polymer stability

(c) This work: Transition metal-catalyzed dearomatization polymerization

- Easy-to-obtain non-spiro monomers
- One-pot spiro-polymerization
- High catalytic efficiency
- Mild conditions

Scheme S1. Methods to access spiropolymers: Step-coupling from pre-synthesized spiro-monomers (a); Polycondensation between non-spiro monomers (b); and transition metal-catalyzed step-growth polymerization of azido salts and diynes (c).

Among the library of polymers, spirocyclic polymers with interesting 3D structures have been an intriguing synthetic target due to their broad application in organic light-emitting devices, drug carriers and gas storage. The introduction of spiral ring in the polymer chain can bring about great change to polymer property, including high thermal and chemical properties, spiroconjugation and heterohead effects,[1] rendering the corresponding spiro-

5

polymer with fascinating photophysical properties, stimulated responsive properties and micropore characteristics.[2] The conventional approach to access spiropolymers concentrated on the condensation polymerization based on presynthesized spiro-monomers(**Scheme S1a**).[3, 4] However, these methods generally suffer from tedious reaction steps, harsh polymerization conditions, complexities in incorporating multiple substituents, and a shortage of suitable monomers. To date, there is only limited method to generate spiropolymers from non-spiro substrates, which usually require well-designed bifunctional substrates(**Scheme S1b**).[5, 6] Therefore, the development of facile polymerization methods for the *in-situ* generation of spiro-polymers from commercially available or readily accessible monomers is thus of great interest.

Over the past few years, dearomatization of phenols has developed as a powerful strategy to access three-dimensional structures. Specifically, by employing phenol derivatives and alkyne coupling partners as reactants, a diverse range of three-dimensional spiro-[4,5]cyclohexadienone products can be successfully obtained through a one-pot dearomatized spiroannulation.[7] Importantly, the resultant spiro-[4,5]-cyclohexadiene-8-one moiety featuring carbonyl-activated carbon-carbon double bonds, may serve as potent photoresponsive skeletons, which display spatial and temporal control for output signal. (**Scheme S1c**)

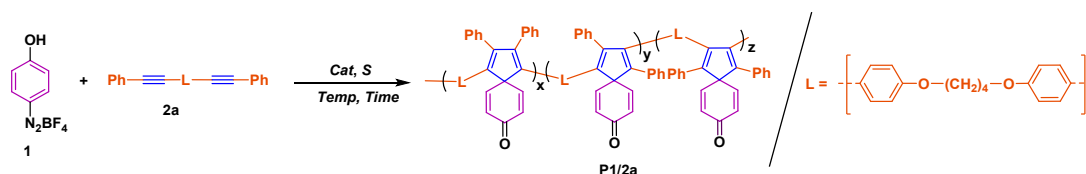# 3. Optimization of the reaction conditions

Table S1. Effect of solvent and temperature on the polymerization of 1a and 2a.[a]

Entry	Solvent	Temp (℃)	Yield (%)	M_w^c	M_n^c	$Đ^c$
1	MeOH	20	/	/	/	/
2	MeOH	40	/	/	/	/
3	DCM	40	/	/	/	/
4	DCM:MeOH[b] = 1:1	20	53	4100	1200	3.4
5	DCM:MeOH = 1:1	40	54	5300	1600	3.3
6	DCM:MeOH = 1:1	60	41	4800	1400	3.4
7	DCE:MeOH = 1:1	70	48	4100	2400	1.7
8	Diox: MeOH = 1:1	80	35	4000	1800	2.2
9	DMF: MeOH = 1:1	100	18	3500	2000	1.8

[a] Carried out under nitrogen for 12 h in the presence of Pd(OAc)$_2$ = 5 mmol %, [1a]/[2a](M) = 0.1/0.1; [b] DCM/MeOH with 1/1 vol. ratio was used as the solvent. [c] Determined by GPC in THF on the basis of a polymethyl methacrylate calibration. $Đ$ = polydispersity = M_w/M_n.
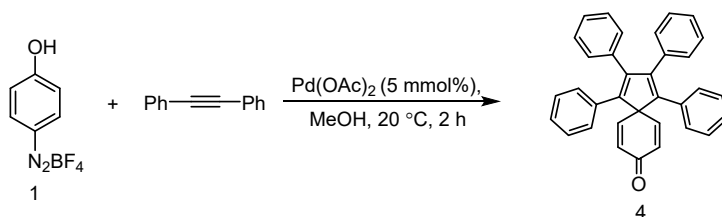
Table S2. Effect of monomer concentration on the polymerization of 1a and 2a.[a]

Entry	[1a]/[2a](M)	Temp (℃)	Yield (%)	M_w^b	M_n^b	$Đ^b$
10	0.2/0.1	40	37	4000	2100	1.9
11	0.1/0.2	40	/	/	/	/
12	0.05/0.05	40	53	4500	2700	1.7

# 4. Synthesis and Characterization

Model Compound Synthesis and Characterization

Scheme S1. Preparation of Model Compound 4.

To a dried round-bottom flask (25 mL) was added 4-phenol diazonium tetrafluoroborate tolane (416.1 mg, 2 mmol)、tolane (890.4 mg, 5 mmol) and Pd(OAc)$_2$ (22.5 mg, 0.1 mmol) under air into the atmosphere. After vacuuming the flask and purging it with nitrogen for three times, add dry methanol (8.0 ml) through the syringe and stir the mixture at room temperature for 2 h. After the reaction was complete (monitored with TLC), extraction was performed three times with saturated NH$_4$Cl and DCM. Dry the organic phase with anhydrous Na$_2$SO$_4$ and remove the solvent under reduced pressure. The crude product was purified by flash silica gel column chromatography (DCM:PE = 1:1) to obtain the desired yellow solid. (720 mg 80.4% yield). ^{1}H NMR (400 MHz, Chloroform-*d*) δ 7.19 – 7.02 (m, 16H), 6.94 – 6.87 (m, 4H), 6.85 – 6.78 (m, 2H), 6.48 – 6.39 (m, 2H). ^{13}C NMR (101MHz, Chloroform-*d*) δ 186.13, 147.86, 147.61, 141.26, 134.66, 134.53, 131.85, 129.94, 129.31, 127.96, 127.88, 127.46, 127.27, 66.23. IR (KBr): 3056, 2926, 1659, 1600, 1496, 1442, 863, 785, 757, 740, 714, 693 cm^{-1}. HRMS (ESI) m/z calculated for C$_{34}$H$_{24}$O [M+Na]$^+$ 471.1719, found 471.1710.

Polymer Synthesis and Purification:
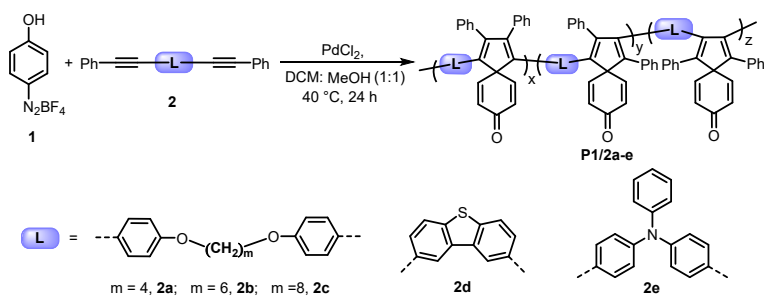
Scheme S2. Preparation of P1/2a-e.

General procedure for the preparation of **P1/2a-e**:

Into a 10 mL schlenk tube with a stirring bar was added 4-phenol diazonium tetrafluoroborate **1** (20.8 mg, 0.1 mmol), internal diyne **2** (0.1 mmol), PdCl₂ (1.78 mg, 10 mmol%), in a mixture of 0.5 mL DCM and 0.5 mL MeOH. The reaction mixture was stirred under nitrogen at 40 °C for 48 h. The resulting mixture is diluted with 5ml methylene chloride (DCM) and filtered. Under intense agitation, the filtered organic phase was dropped into 80 mL of hexane/chloroform mixture (7:1 v/v). The sediment was filtered and collected, washed with n-hexane, and dried to a fixed weight by vacuum at room temperature.The structural characterization results were summarized as follows:

P1/2a: brown powder; yield: 93.7% (**Table 2, entry 1**). M_w: 27400; M_n: 16400; M_w/M_n: 1.7 (GPC, PMMA calibration). ¹H NMR (400 MHz, Chloroform-d) δ (ppm): 7.13–7.01, 6.98–6.85, 6.81–6.72, 6.64–6.56, 6.46–6.36, 3.90, 1.90. ¹³C NMR (101 MHz, CD₂Cl₂,) δ (ppm): 186.39, 158.11, 148.65, 147.30, 146.97, 140.09, 135.11, 134.90, 131.59, 131.28, 131.22, 130.47, 130.04, 129.98, 129.34, 127.96, 127.27, 127.11, 126.95, 113.89, 67.26, 66.19, 66.13, 31.59, 26.00, 22.66, 14.13. IR (KBr): 3051, 2923, 2870, 1656, 1604, 1507, 1244, 1175, 1073, 834, 736, 698 cm⁻¹.

P1/2b: brown powder; yield: 89.2 % (**Table 2, entry 2**). M_w: 24100; M_n: 13300; M_w/M_n: 1.8 (GPC, PMMA calibration). ¹H NMR (400 MHz, Chloroform-d) δ (ppm): 7.14–7.02, 7.00–6.86, 6.83-6.73, 6.66–6.57, 6.48–6.37, 3.88, 1.77, 1.50. ¹³C NMR (101 MHz, CD₂Cl₂,) δ (ppm): 186.44, 158.22, 148.75, 147.37, 146.97, 135.13, 134.92, 131.55, 131.26, 131.20, 130.44, 130.04, 129.35, 127.95, 127.25, 127.09, 126.85, 113.88, 67.66, 66.20, 31.59, 29.21, 25.90,

22.66, 14.13. IR (KBr): 3052, 2934, 2863, 1657, 1605, 1508, 1442, 1246, 1175, 836, 735, 699 cm^{-1}.

P1/2c: brown powder; yield: 73.9% (**Table 2, entry 3**). M_w: 16000; M_n: 7300; M_w/M_n: 2.2 (GPC, PMMA calibration). ^{1}H NMR (400 MHz, Chloroform-d) δ (ppm): 7.13–7.01, 6.98–6.88, 6.82–6.73, 6.61, 6.41, 3.87, 1.74, 1.42, 1.36. ^{13}C NMR (101 MHz, CD$_2$Cl$_2$,) δ (ppm): 187.10, 158.25, 148.81, 147.40, 139.88, 135.13, 134.91, 132.28, 131.52, 131.25, 131.19, 130.42, 130.05, 129.98, 129.34, 127.95, 127.65, 127.24, 127.08, 126.78, 113.89, 67.78, 29.29, 26.01, 22.67. IR (KBr): 3055, 2930, 2856, 1657, 1604, 1461, 1441, 1247, 1176, 1028, 835, 764, 699 cm^{-1}.

P1/2d: brownish yellow powder; yield: 65.5 % (**Table 2, entry 4**). M_w: 7900; M_n: 3400; M_w/M_n: 2.3 (GPC, PMMA calibration). ^{1}H NMR (400 MHz, Chloroform-d) δ (ppm): 8.05, 7.81–7.73, 7.56, 7.35, 7.12, 7.01–6.93, 6.88, 6.54–6.42. ^{13}C NMR (101 MHz, CD2Cl2,) δ (ppm): 186.35, 148.10, 138.90, 135.04, 131.71, 130.98, 130.06, 129.57, 128.52, 128.28, 122.63, 115.60, 77.44. IR (KBr):3050, 2920, 2851, 1657, 1594, 1394, 1231, 1083, 1023, 818, 751, 698 cm^{-1}.

P1/2e: Light brown powder; yield: 75.8 % (**Table 2, entry 5**). M_w: 4500; M_n: 2600; M_w/M_n: 1.7 (GPC, PMMA calibration). ^{1}H NMR (400 MHz, Chloroform-d) δ (ppm): 8.04, 7.82, 7.48, 7.15–7.03, 6.77, 6.42. ^{13}C NMR (101 MHz, CD$_2$Cl$_2$) δ (ppm): 186.07, 146.89, 132.62, 131.54, 130.99, 129.45, 128.70, 128,39, 128.02,126.79, 115.55, 77.39. IR (KBr): 3032, 2923, 1713, 1656, 1589, 1503, 1321, 1275, 1173, 764, 750 cm^{-1}.
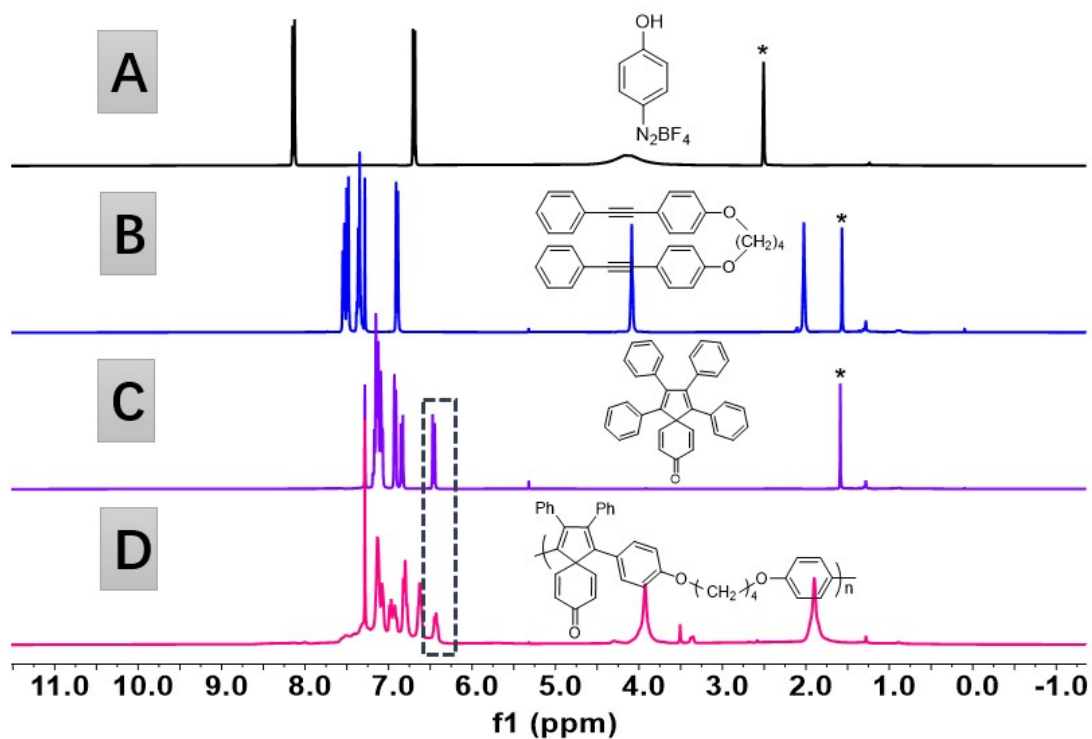
5. ¹H NMR spectra of spiropolymers

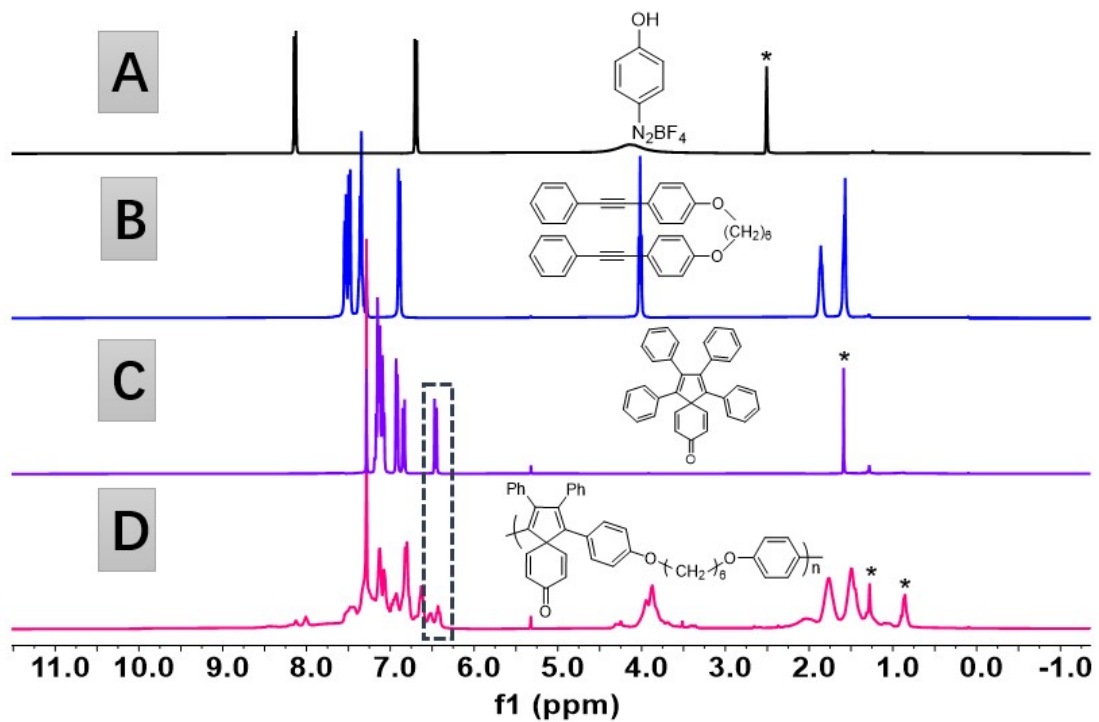**Figure S1.** ¹H NMR spectra of (A) **1**, (B) **2a**, (C) **4** (D) **P1/2a**.

Figure S2. ^{1}H NMR spectra of (A) **1**, (B) **2b**, (C) **4**, (D) **P1/2b**.
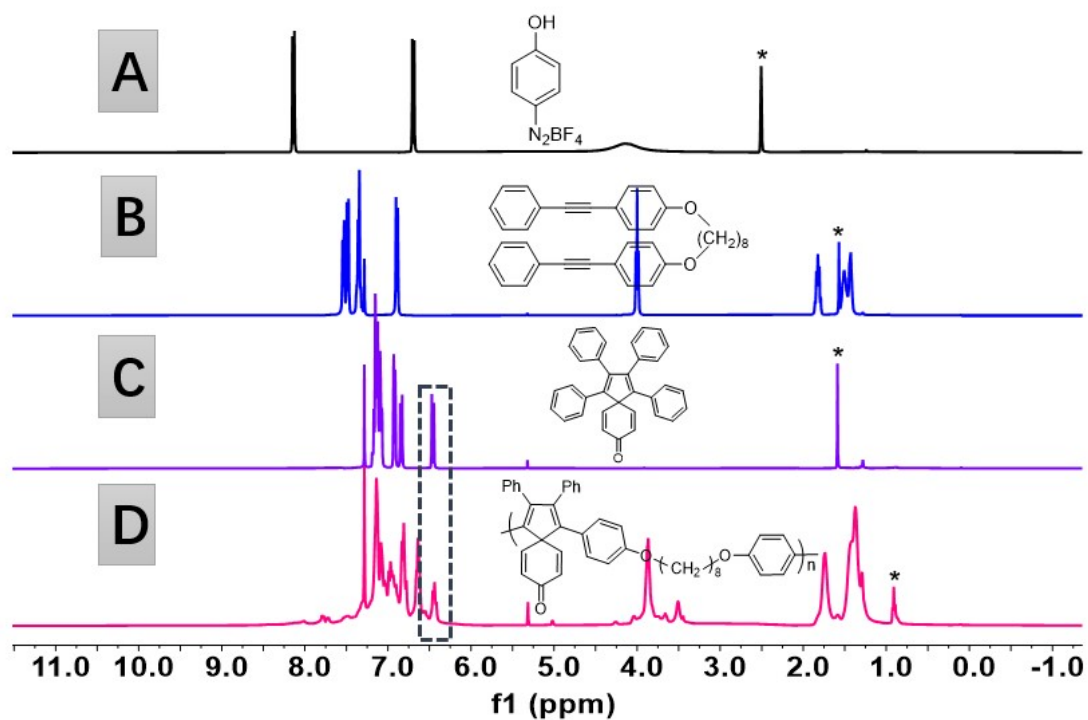

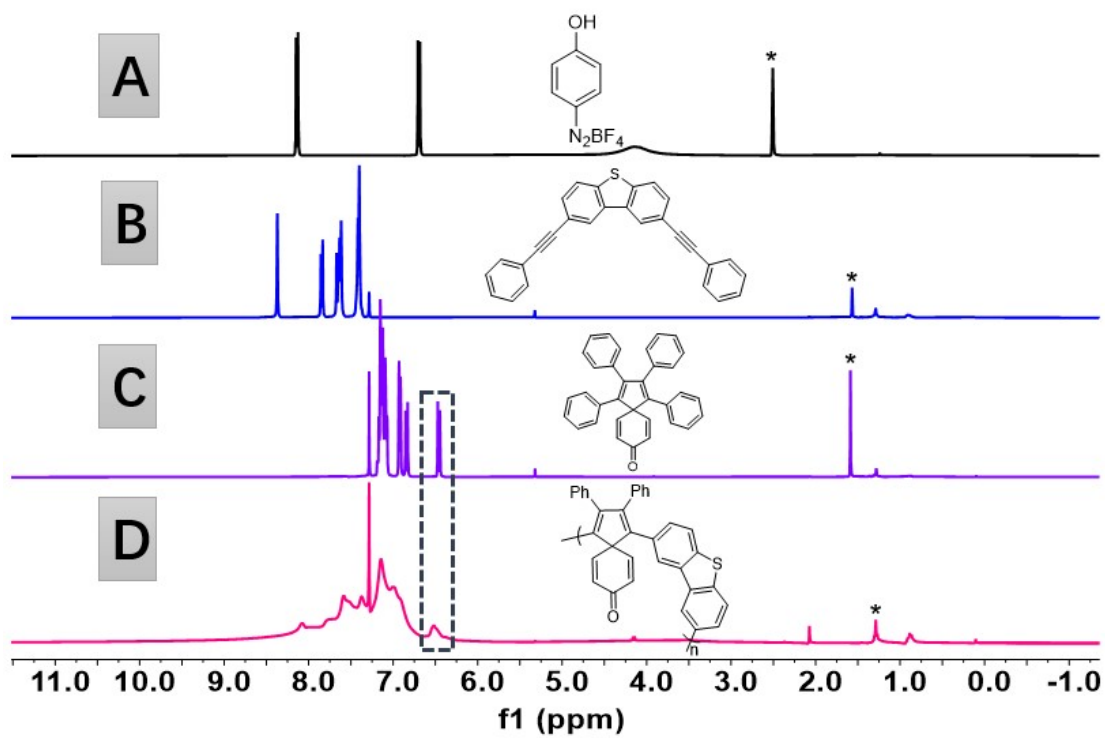**Figure S3.** ^{1}H NMR spectra of (A) **1**, (B) **2c**, (C) **4**, (D) **P1/2c**.

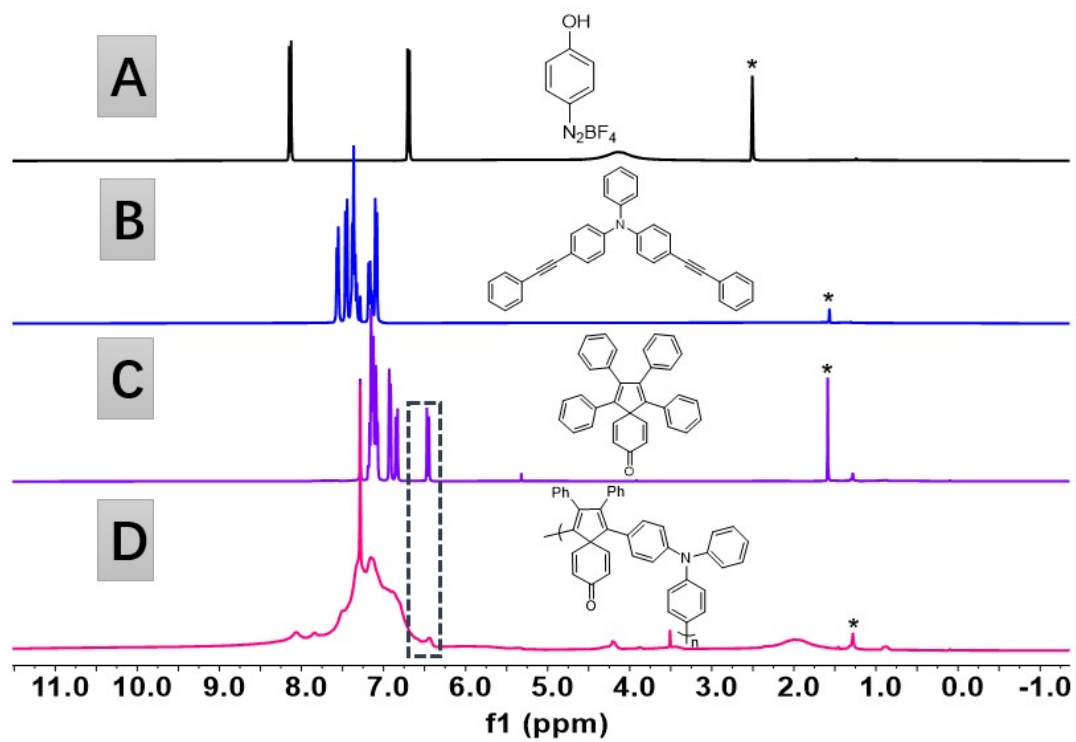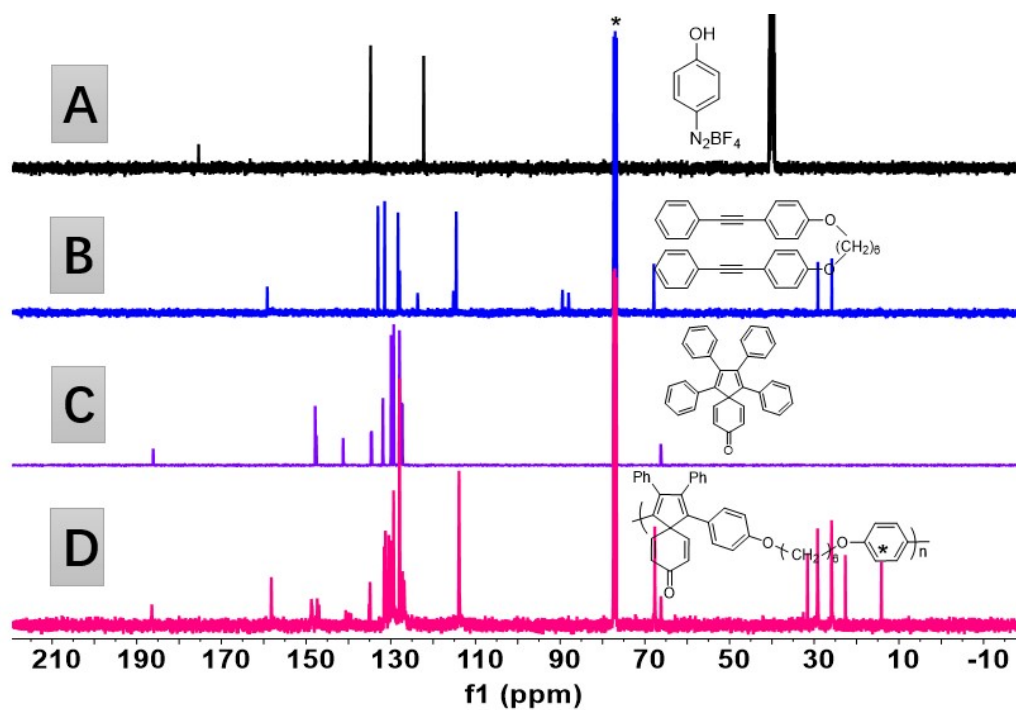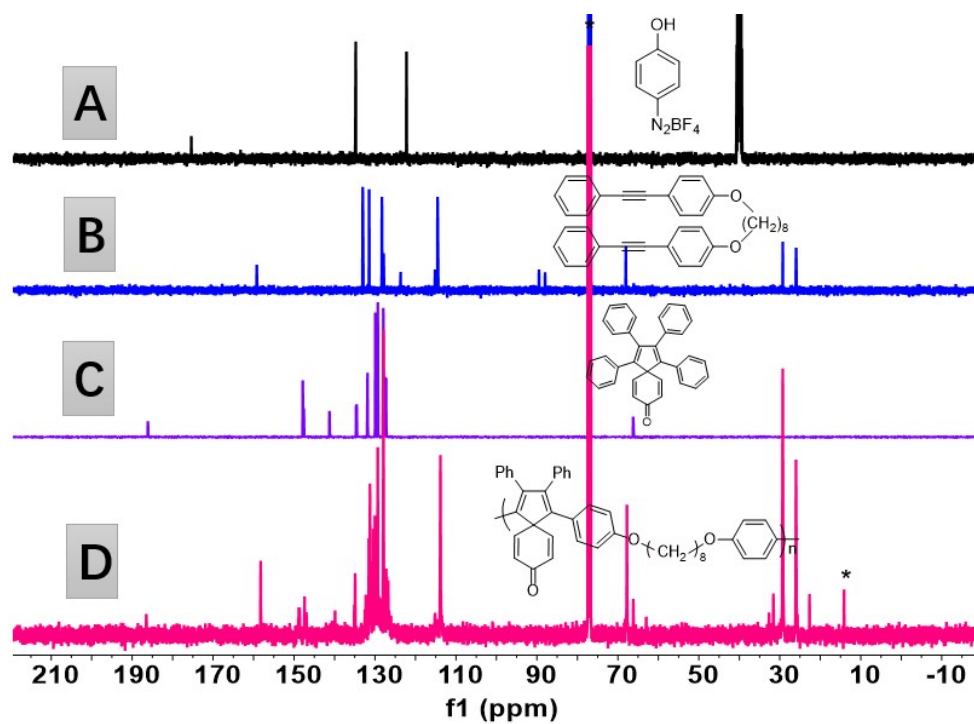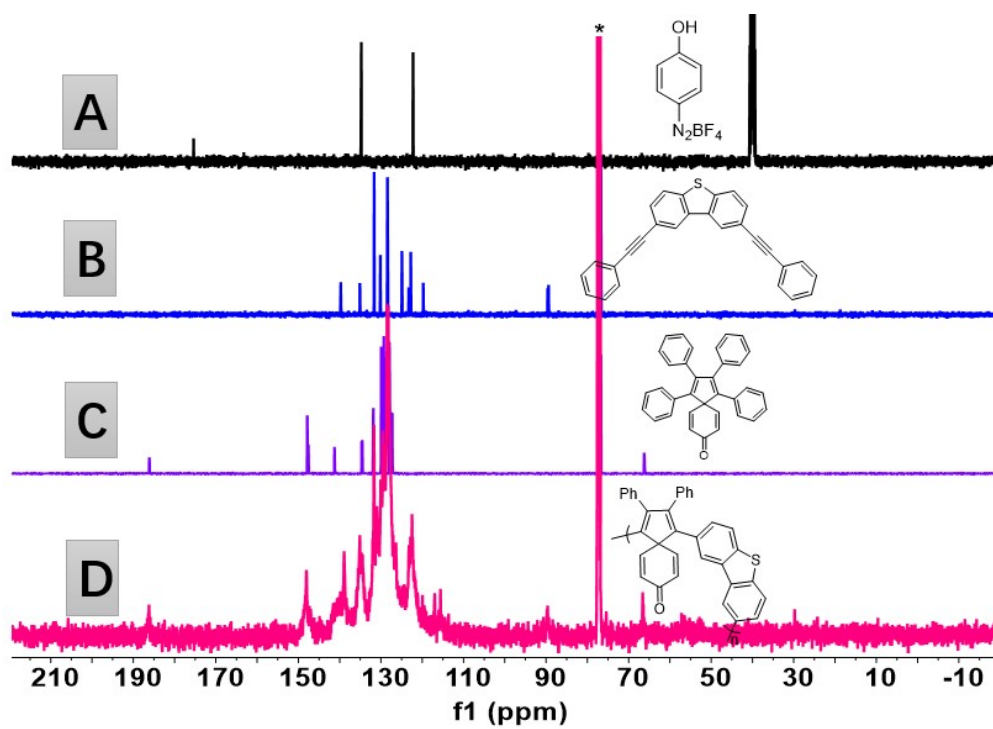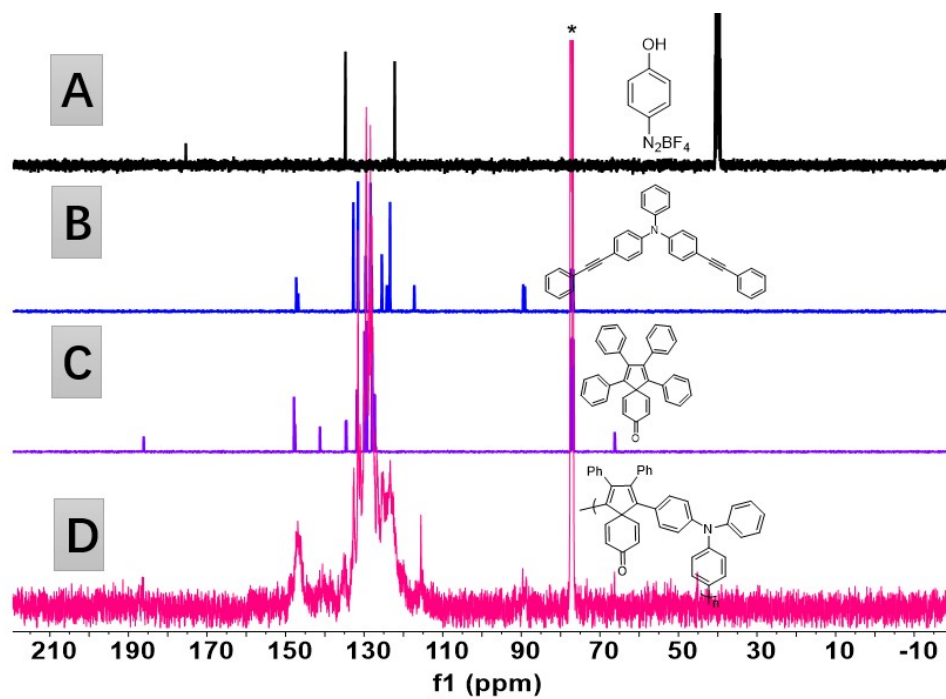**Figure S4.** ^{1}H NMR spectra of (A) **1**, (B) **2d**, (C) **4**, (D) **P1/2d**.

Figure S5. ^{1}H NMR spectra of (A) **1**, (B) **2e**, (C) **4**, (D) **P1/2e**.

6. ¹³C NMR spectra of spiropolymers
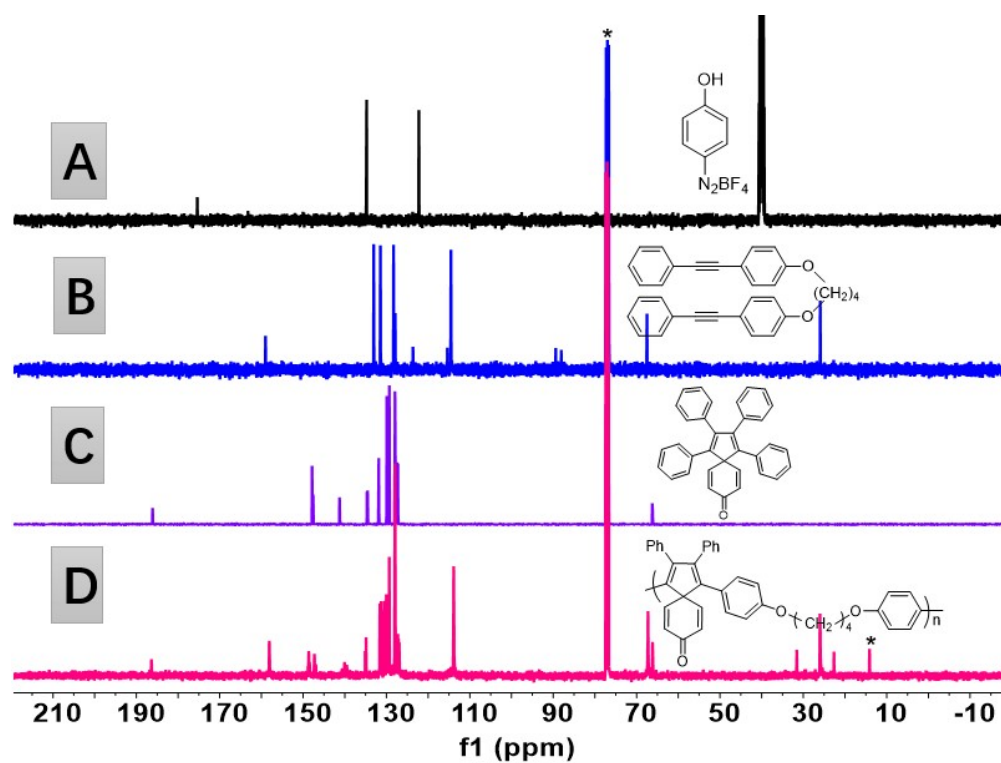
Figure S6. ¹³C NMR spectra of (A) **1**, (B) **2a**, (C) **4**, (D) **P1/2a**.

Figure S7. ^{13}C NMR spectra of (A) **1**, (B) **2b**, (C) **4,** (D) **P1/2b**.

Figure S8. ^{13}C NMR spectra of (A) **1**, (B) **2c**, (C) **4,** (D) **P1/2c**.

Figure S9. ^{13}C NMR spectra of (A) **1**, (B) **2d**, (C) **4**, (D) **P1/2d**.

Figure S10. ^{13}C NMR spectra of (A) **1**, (B) **2e**, (C) **4**, (D) **P1/2e**.
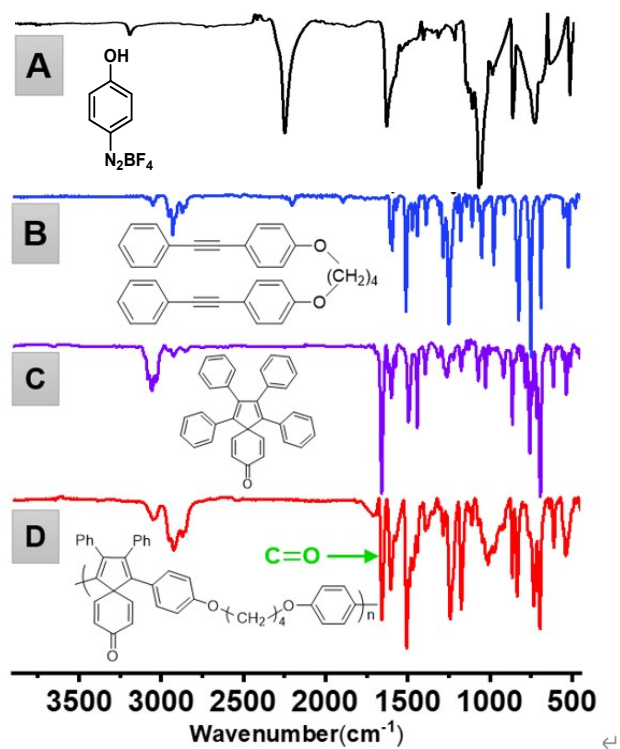
7. FT-IR spectra of spiropolymers

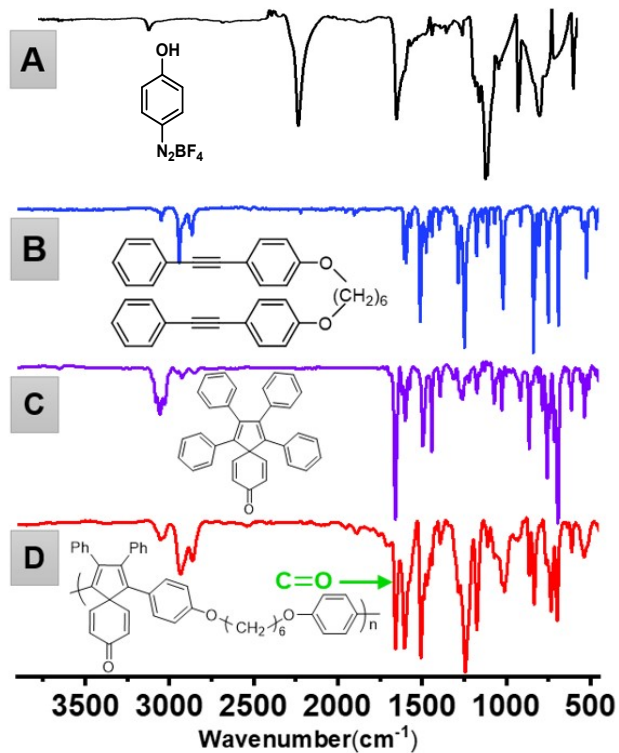**Figure S11.** FT-IR spectra of (A) **1**, (B) **2a**, (C) **4**, (D) **P1/2a**.

Figure S12. FT-IR spectra of (A) **1**, (B) **2b**, (C) **4**, (D) **P1/2b**.
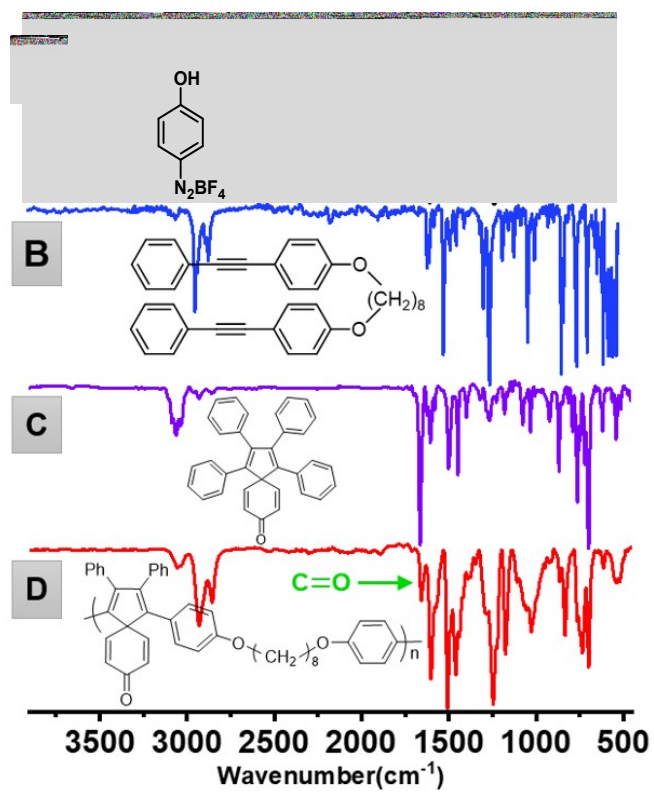
Figure S13. FT-IR spectra of (A) **1**, (B) **2c**, (C) **4**, (D) **P1/2c**.
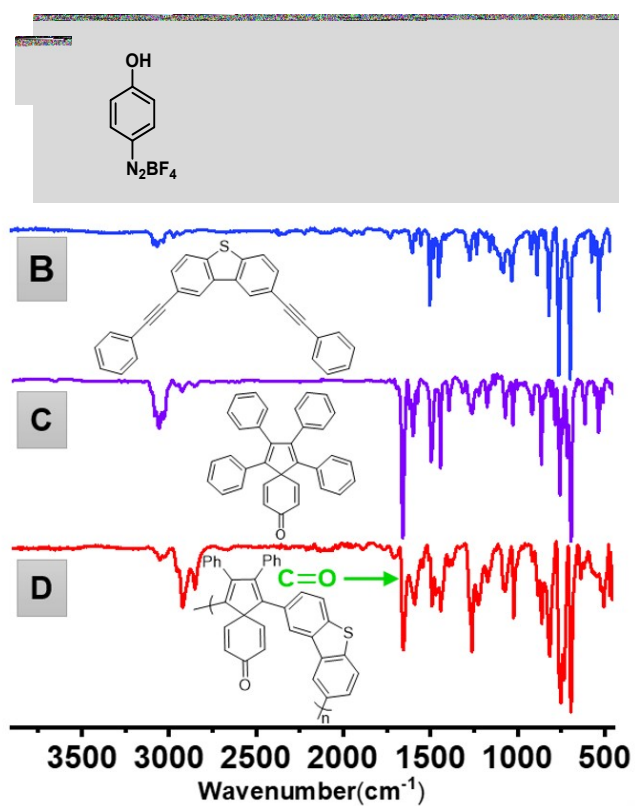
Figure S14. FT-IR spectra of (A) **1**, (B) **2d**, (C) **4**, (D) **P1/2d**.
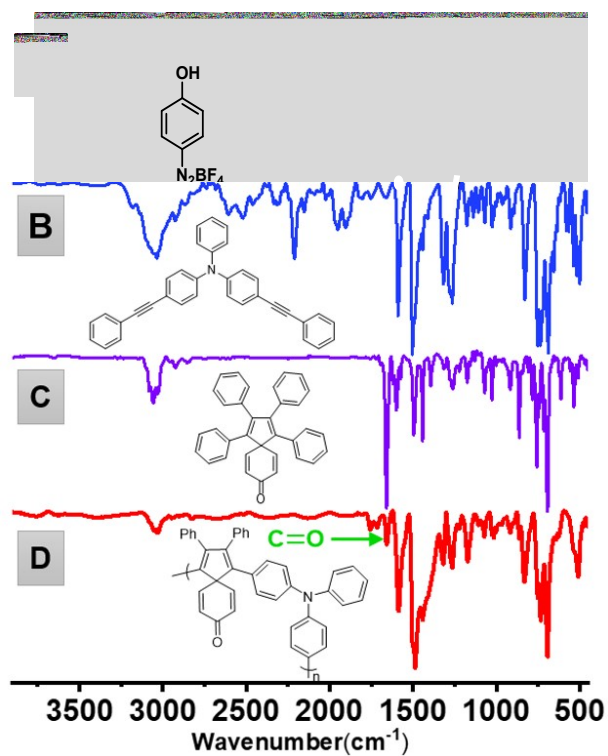
Figure S15. FT-IR spectra of (A) **1**, (B) **2e**, (C) **4**, (D) **P1/2e**.

8. Solubility of P1/2(a-e)

Table S3. Solubility of P1/2(a-e).

	DMA	DMSO	Diox	MeOH	EA	NMP	Tol	THF	MeCN	MTBE	TCM
P1/2a	☞	☞	☞	⎘	①	☞	①	☞	①	⎘	☞
P1/2b	☞	☞	☞	⎘	①	☞	①	☞	①	⎘	☞
P1/2c	☞	☞	☞	⎘	①	☞	①	☞	①	⎘	☞
P1/2d	☞	☞	☞	⎘	⎘	☞	①	☞	⎘	⎘	☞
P1/2e	☞	☞	☞	⎘	①	☞	①	☞	①	⎘	☞

Key: "☞"completely soluble at room temperature; "①"slightiy soluble at refluxing; "⎘" insoluble at refluxing; NMP stands for N-Methyl-2-pyrrolidinone; MTBE stands for Methyl Tertiary Butyl Ether.
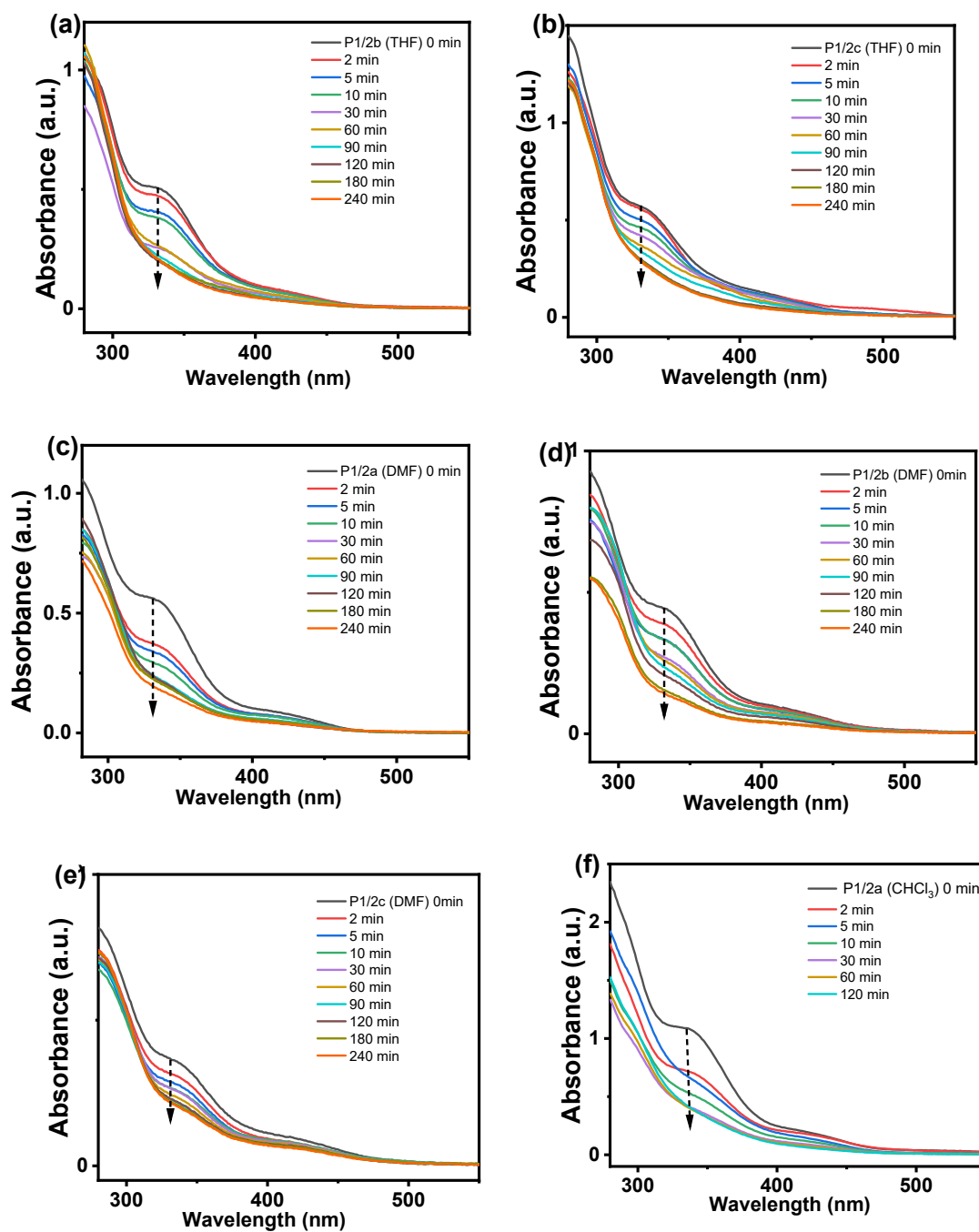
9. UV irradiation experiment

Figure S16. UV−vis spectra of **P1/2b** (a) and**P1/2c** (b) in THF irradiated by UV light for different times; UV−vis spectra of **P1/2a** (c)**, P1/2b** (d) and **P1/2c** (e) in DMF irradiated by UV light for different times; UV−vis spectra of **P1/2a** (e) in CHCl$_3$ irradiated by UV light for different times.
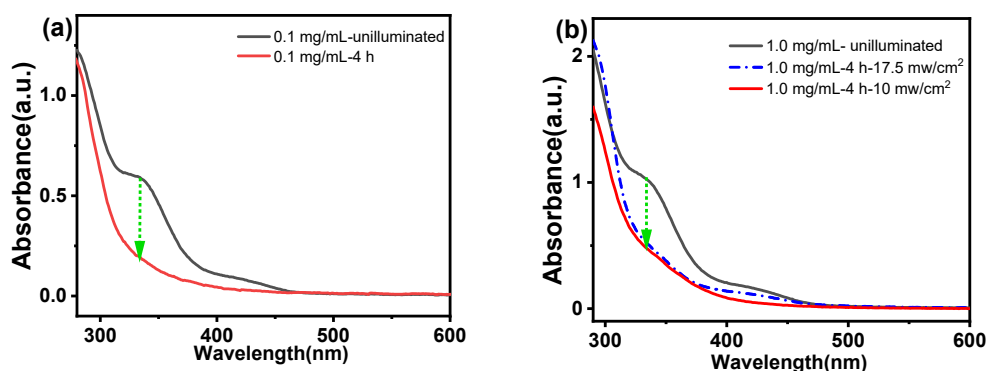
Figure S17. (a) UV-vis spectra of **P1/2a** at 0.1 mg/mL concentration in THF without irradiation (black) and after 4 hours of UV irradiation (red, 10 mw/cm^2); (b) UV-vis spectra of **P1/2a** at a concentration of 1.0 mg/mL in THF unilluminated (black) and after 4 hours of UV irradiation(blue, 17.5 mw/cm^2; red, 10 mw/cm^2).

The degree of crosslinking (x) was calculated by the equation $x = 1 - (A_t/A_0)$ was estimated to be ~67% (**Figure S17a**). When the radiation concentration had been increased from 0.1 mg/mL to 1.0 mg/mL, the crosslinking degree had remained at $x = 53\%$, indicating that an increase in concentration had not enhanced the crosslinking degree. Furthermore, after having attempted to increase the illuminance to 17.5 mw/cm², the crosslinking degree had decreased to $x = 49\%$, suggesting that an increase in illuminance had not led to an increase in the crosslinking degree. (**Figure S17b**)
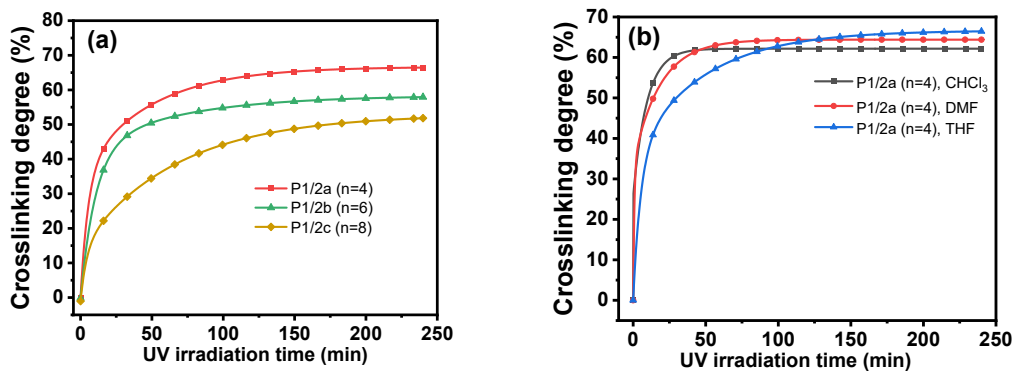
Figure S18. (a) Plots of crosslinking degrees of **P1/2a-c** vs UV irradiation times in THF solvents; (b) Plots of crosslinking degrees of **P1/2a** (n=4) vs UV irradiation times in different solvents.
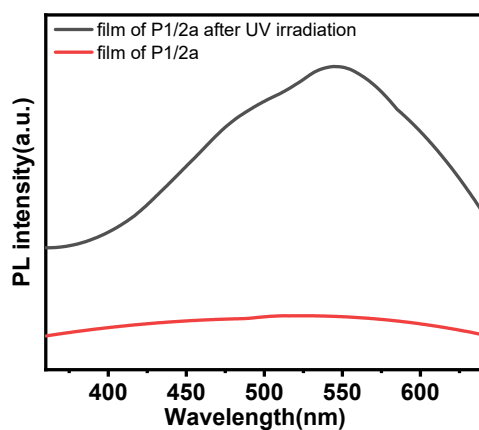

Figure S19. PL spectra of the drop-casting thin film of **P1/2a** before and after UV irradiation.

Table S4. Fluorescence quantum yield of **P1/2a**.

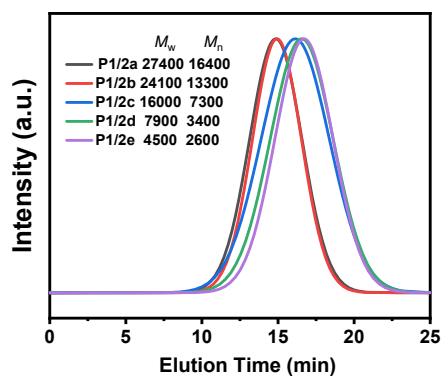|	CHCl$_3$	DMF	THF	Solid Film
Before UV	5.3%	3.7%	3.6%	Not detected
After UV	11.4%	10.8%	13.9%	13.2%

10. GPC data of spiropolymers

Figure S20. Overlay of the GPC traces of the polymers reported. (Estimated by GPC in THF on the basis of Polymethyl methacrylate calibration).
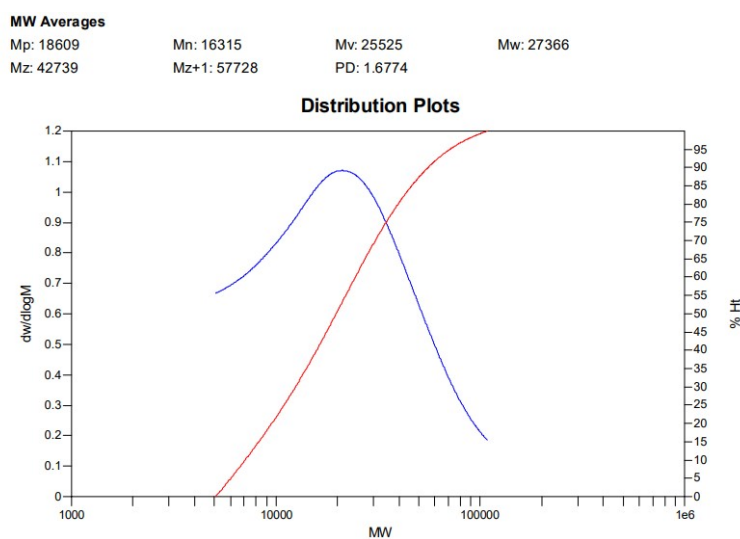

Figure S21. GPC curves of P1/2a

MW Averages

Mp: 17335   Mn: 13342   Mv: 22272   Mw: 24090
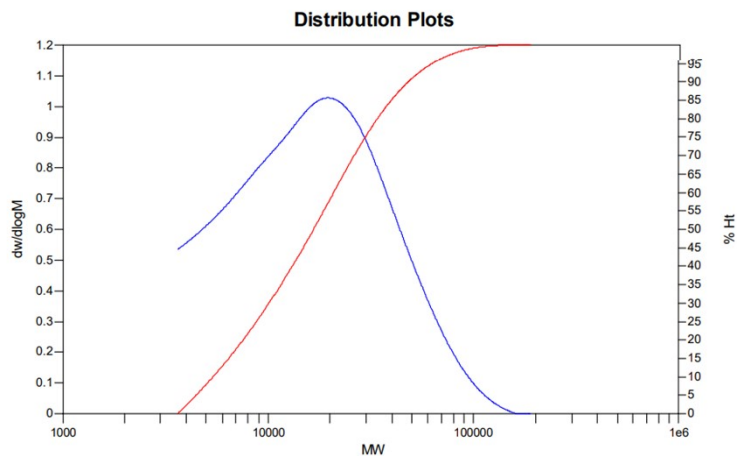
Mz: 40000   Mz+1: 57643   PD: 1.8056

Distribution Plots

Figure S22. GPC curves of P1/2b

MW Averages

Mp: 4785   Mn: 7274   Mv: 14329   Mw: 16026

Mz: 32463   Mz+1: 50874   PD: 2.2032

Distribution Plots

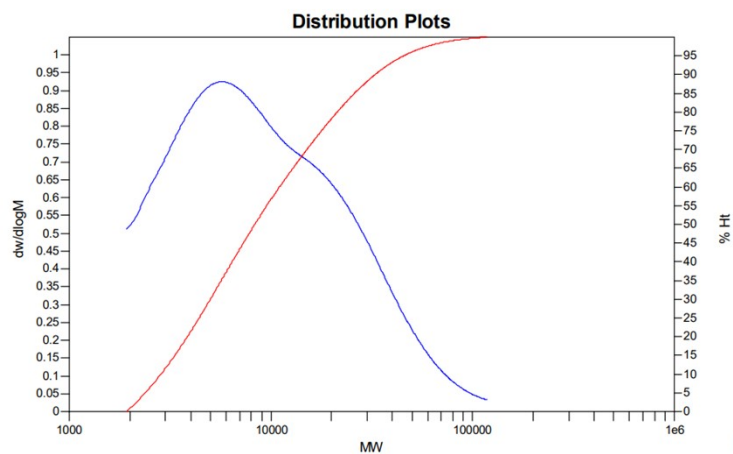

Figure S23. GPC curves of P1/2c

MW Averages

Mp: 3303   Mn: 3428   Mv: 7121   Mw: 7967

Mz: 16740   Mz+1: 29172   PD: 2.3241
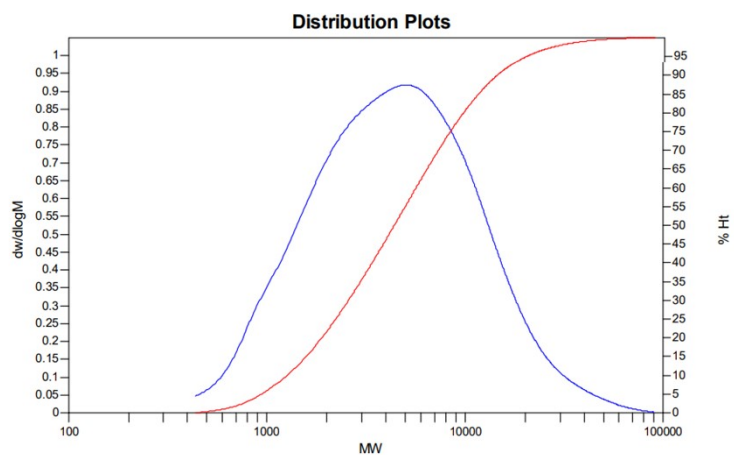

Figure S24. GPC curves of P1/2b

MW Averages

Mp: 2648   Mn: 2600   Mv: 4221   Mw: 4520

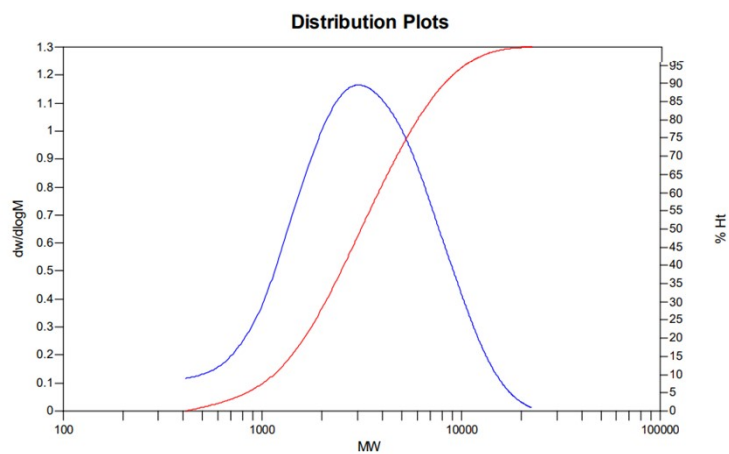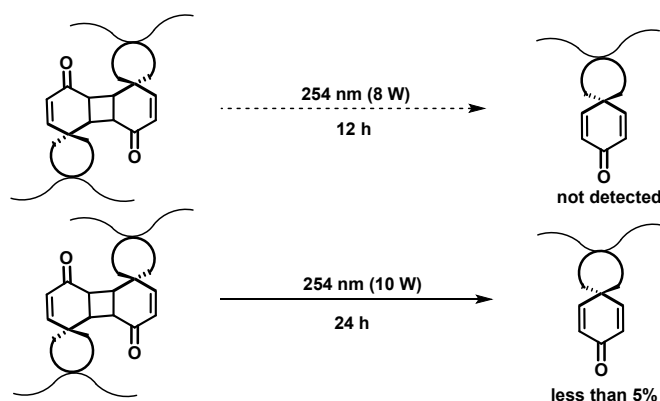Mz: 6999   Mz+1: 9543   PD: 1.7385

Figure S25. GPC curves of P1/2e

11. UV-254 nm irradiation for decrosslinking

Initially, we conducted the de-crosslinking experiment through exposing the photodimers of P1/2a under UV irradiation (254 nm, 8W) for 12 h, however, we can't obtain any de-crosslinking monomers. Then, we increased the irradiation energy (UV lamp, 254 nm) to 10 W and the explosion time to 24 h, and found that less than 5% of the covalent bond breaks (evaluated from the mass loss), so we still deduced its irreversibility as the broken proportion is few. Through literature survey, we concluded the main reasons for the differences in reversibility for such [2+2] photochemical reactions compared to coumarins are possibly as follows:

Firstly, the crosslinking degree of [2+2] cycloaddition for our system is around 70%. When the crosslinked product was irradiated under UV, more energy will be competitively absorbed by the uncrosslinked P1/2a (as shown in Figure S17) due to their higher degree of conjugation (25%). In this situation, the competitive absorption of the spiro-polymer is one reason leading to the irreversibility of the crosslinking process.[8]

Additionally, despite the spirocyclic polymer in this paper possesses similar α, β-unsaturated double bonds as the reversible monomers, such as coumarin or cinnamic acid, the spirocycle existence may cause high degree plane rotation above the spiro carbon due to the formation of cyclobutane ring between the carbonyl activated double bonds.[9] We deduced that such high degree of structural reorganization and the establishment of a highly rigid and photostable structure is another reason contributing to the irreversibility of this reaction. After all, to destroy such a rigid structure would likely require higher energies for greater restructuring.

(1) Yu, S.; Li, S.; Liu, Y.; Cui, S.; Shen, X. High-performance microporous polymer membranes prepared by interfacial polymerization for gas separation. *J. Membr. Sci.* **2019**, *573,* 425-438.

(2) Wright, I. A.; Kanibolotsky, A. L.; Cameron, J.; Tuttle, T.; Skabara, P. J.; Coles, S. J.; Howells, C. T.; Thomson, S. A. J.; Gambino, S.; Samuel, I. D. W. Oligothiophene Cruciform with a Germanium Spiro Center: A Promising Material for Organic Photovoltaics. *Angew. Chem., Int. Ed.* **2012**, *51,* 4562-4567.

(3) Schmidt, S. B.; Kempe, F.; Brügner, O.; Walter, M.; Sommer, M. Alkyl-substituted spiropyrans: electronic effects, model compounds and synthesis of aliphatic main-chain copolymers. *Polym. Chem.* **2017**, *8,* 5407-5414.

(4) Valero, S.; Collavini, S.; Völker, S. F.; Saliba, M.; Tress, W. R.; Zakeeruddin, S. M.; Grätzel, M.; Delgado, J. L. Dopant-Free Hole-Transporting Polymers for Efficient and Stable Perovskite Solar Cells. *Macromolecules.* **2019**, *52,* 2243-2254.

(5) Zhao, Y.; Zhang, L.; Wang, T.; Han, B. Microporous organic polymers with acetal linkages: synthesis, characterization, and gas sorption properties. *Polym. Chem.* **2014**, *5,* 614-621.

(6) Lee, Y. G.; Kang, S.; Moerdyk, J. P.; Bielawski, C. W. Poly(2-imino-4-oxazolidinone)s via the Condensation of Diamidocarbenes with Bis(isocyanate)s. *Macromolecules.* **2015**, *48,* 9081-9084.

(7) Schmidt, B.; Berger, R.; Kelling, A.; Schilde, U. Pd-Catalyzed [2+2+1] Coupling of Alkynes and Arenes: Phenol Diazonium Salts as Mechanistic Trapdoors. *Chem. Eur. J.* **2011**, *17,* 7032-7040.

(8) Chambers, L. C.; Barner-Kowollik, C.; Barner, L.; Michalek, L.; Frisch, H. Photostationary State in Dynamic Covalent Networks. *ACS Macro. Lett.* **2022**, 11, 532-536

(9) Aljuaid, M.; Chang, Y.; Haddleton, D. M.; Wilson, P.; Houck, H. A. Thermoreversible [2+ 2] Photodimers of Monothiomaleimides and Intrinsically Recyclable Covalent Networks Thereof. *J. Am. Chem. Soc.*, **2024**, 146, 19177-19182